Available online at www.sciencedirect.com
ScienceDirect
Scripta Materialia 63 (2010) 1205–1208
Scripta MATERIALIA
www.elsevier.com/locate/scriptamat

Room temperature creep in amorphous alloys: Influence of initial strain and free volume

Byung-Gil Yoo,[a] Kyu-Sik Kim,[a] Jun-Hak Oh,[a] U. Ramamurty[b] and Jae-il Jang[a,*]

[a] *Division of Materials Science and Engineering, Hanyang University, Seoul 133-791, Republic of Korea*
[b] *Department of Materials Engineering, Indian Institute of Science, Bangalore 560012, India*

Received 3 August 2010; accepted 18 August 2010
Available online 24 August 2010

The role of imposed strain on the room temperature time-dependent deformation behavior of bulk metallic glasses (BMGs) was systematically investigated through spherical nanoindentation creep experiments. The results show that creep occurred even at very low strains within elastic regimes and, interestingly, a precipitous increase in creep rate was found in plastic regimes, with BMG that had a higher free volume exhibiting greater creep rates. The results are discussed in terms of prevailing mechanisms of elastic/plastic deformation of amorphous alloys.

Keywords: Metallic glasses; Creep; Nanoindentation; Free volume

The plastic deformation behavior of amorphous alloys has been an active area of research for the last several decades [1–3]. At relatively low temperatures and high stresses plastic flow tends to localize into 'shear bands'. At high temperatures (above ~0.7 T_g, where T_g is the glass transition temperature) homogeneous deformation occurs through shear-mediated strain accommodation by clusters of atoms referred to as shear transformation zones (STZs), which are aided by the free volume that is available in the material [1–3].

Recently many studies [4–14] have focused on the time-dependent deformation or creep behavior of bulk metallic glasses (BMGs). The results showed that creep in BMGs was mostly homogeneous [5]. Importantly, the results showed that BMGs can creep even at room temperature [8,9,12–14]. For some BMGs (such as Ce-, La- and Mg-based glasses [8,9]) room temperature is itself ~0.70–0.75 T_g and, hence, the observation of creep was not surprising. However, it was noted even for Fe- and Ti-based BMGs, whose T_g is not so low [12,13].

The room temperature creep behavior of amorphous alloys has been examined under either unaxial compression [7,10,11] or sharp indentation [8,9,12–14]. While a uniform stress state prevails in uniaxial tests, the applied stress cannot exceed the yield strength σ_y of the alloy. This is due to the fact that the specimen is likely to become unstable once the stress exceeds σ_y. In nanoindentation experiments with a sharp tip (e.g. the commonly used Berkovich or Vickers indenters) the imposed strains are fixed (and typically large) within plastic regimes and independent of load due to the geometrical self-similarity of the indenters. In addition, as the material underneath the indenter experiences plastic constraint, the results obtained from it cannot be directly compared with those obtained through uniaxial tests. Therefore, it is difficult to systematically analyze the influence of the initial stress or strain level on the creep behavior of BMGs over a wide range of imposed conditions that span elastic to plastic regimes of deformation.

One of the possible ways to overcome this difficulty is through nanoindentation creep experiments with a spherical indenter. In this technique the indentation strain ε_i (i.e. the equivalent or averaged strain comparable with the strain produced during uniaxial testing) at the onset of creep can be systematically varied by simply changing the applied peak load P_{max} (with a fixed indenter tip radius R). Using the expanding cavity analogy, Johnson [15] determined that $\varepsilon_i = 0.2(a/R)$ for spherical indentation, where a is the contact radius. Thus, increasing P_{max} leads to an increase in ε_i from elastic to elasto-plastic and then to fully plastic regimes. This feature is exploited in this work wherein the influence of ε_i on the time-dependent deformation behavior of $Cu_{50}Zr_{50}$ ($T_g = 693$ K) and $Cu_{65}Zr_{35}$ ($T_g = 750$ K) was investigated. While the former has the lowest atomic packing density among

* Corresponding author. E-mail: jijang@hanyang.ac.kr

1359-6462/$ - see front matter © 2010 Acta Materialia Inc. Published by Elsevier Ltd. All rights reserved.
doi:10.1016/j.scriptamat.2010.08.034

the various bulk forming Cu–Zr binary alloys, $Cu_{65}Zr_{35}$ has the highest [10]. Conversely, $Cu_{50}Zr_{50}$ has highest amount of free volume, while $Cu_{65}Zr_{35}$ has the lowest. This difference facilitates the comparison of the effect of free volume content on the creep behavior of BMGs.

1 mm diameter rods of both alloys were prepared through Cu mold casting. No crystalline peak was detected in the X-ray diffraction spectra of the specimens (not shown here), indicating that the alloys were fully amorphous. Creep experiments were performed using a Nanoindenter-XP (MTS Corp., Oak Ridge, TN) with a spherical tip of radius $R = 30$ μm, which was estimated by Herzian contact analysis [15] of the indentations made on fused quartz. The samples were loaded to P_{max} at a constant strain rate $(dh/dt)h^{-1}$ of 0.5 s^{-1}, held at P_{max} for 400 s and unloaded. Seven different P_{max} (1, 5, 20, 50, 100, 200 and 500 mN) were applied and 20 experiments were conducted in each case. In all these experiments thermal drift was maintained below 0.05 nm s^{-1}.

Figure 1a exhibits normalized load–displacement (P–h) curves for both the BMGs recorded at various P_{max}. For P_{max} =20 and 50 mN the loading sequence of the P–h curves was completely reversed on unloading, indicating that the deformation was fully elastic. When P_{max} was increased to 100 mN the loading and unloading parts of the P–h curve did not overlap, indicating permanent deformation, which became more pronounced at P_{max} = 200 mN. This observation suggested that yielding under quasi-static loading occurred at P_{max} between 50 and 100 mN. Figure 1b shows the P–h curves obtained at $P_{max} = 1$ mN, the lowest P_{max} used in this work. An increase in displacement h during the holding sequence was seen for both alloys, suggesting that creep occurred even at these low load levels. The observation of permanent displacement even after complete unloading in the indentation creep tests indicated that the observed time-dependent deformation was mainly visco-plastic in nature. To reconfirm that the loading stage of deformation was purely elastic the loading curve was fitted following Hertzian contact theory [15]:

$$P = \frac{4}{3} E_r \sqrt{R} h^{1.5} \tag{1}$$

where E_r is the reduced modulus. With the measured value of E_r the elastic constants of the indented sample could be calculated using

$$\frac{E_s}{1-\nu_s^2} = \left(\frac{1}{E_r} - \frac{1-\nu_i^2}{E_i}\right)^{-1} \tag{2}$$

Here E and ν are the elastic modulus and Poisson's ratio, with the subscripts s and i indicating the sample and the indenter. The tip was made of diamond and hence $E_i = 1141$ GPa and $\nu_i = 0.07$ [16]. By fitting the loading part of the P–h curve according to Eq. (2), the plane strain moduli of the samples $E_s/(1-\nu_s^2)$ were estimated to be ~98 and ~130 GPa for $Cu_{50}Zr_{50}$ and $Cu_{65}Zr_{35}$, respectively, which are consistent with the literature data [17]. Importantly, an excellent fit of Eq. (2) to the data (inset in Fig. 1b) suggests that the loading was indeed elastic at these load levels.

Figure 1c shows the P–h curves obtained during indentation at $P_{max} = 500$ mN, which was the highest load applied in the present work. For this case $\varepsilon_i \approx 0.035$ for $Cu_{50}Zr_{50}$ and 0.033 for $Cu_{65}Zr_{35}$, which are higher than the respective uniaxial yield strain ε_y (0.016 and 0.019) [10]. While creep deformation was obvious for both BMGs, it was more pronounced in $Cu_{50}Zr_{50}$ than in $Cu_{65}Zr_{35}$, unlike in the indentation creep experiments with $P_{max} = 1$ mN, in which the creep displacements were similar in both BMGs.

The depth of penetration of the indenter during the holding sequence Δh ($=h - h_0$, where h_0 is the displacement at the start of the hold at P_{max}) is plotted in Figure 2a and 2b as a function of hold time t for $Cu_{65}Zr_{35}$ and $Cu_{50}Zr_{50}$, respectively. It can be seen that Δh is strongly dependent on P_{max}, i.e. creep displacement increases with increasing P_{max}. It is also noteworthy that the curves are relatively smooth, with a conspicuous absence of the flow serrations (or "pop-ins") typically observed during nanoindentation of metallic glasses [3,18]. This observation clearly indicates that the measured time-dependent deformation was indeed due to homogeneous plasticity. In addition, Δh vs. t curves are parabolic in nature (especially at higher P_{max}), which is somewhat analogous to the creep response generally observed during uniaxial loading consisting of two parts in the early stages: transition (primary) creep and steady-state (secondary) creep.

In Figure 3a the total creep displacement h_{creep} (the value of Δh at 400 s) is plotted as a function of ε_i. In this plot the ε_y values for both alloys are shown as vertical lines, to demarcate elastic and inelastic regimes of deformation. It is evident that h_{creep} is sensitive to ε_i, especially in the plastic regime. However, it should be noted that a direct comparison of h_{creep} values can be misleading, as this does not reflect the difference in the strain state at the onset of creep. This calls for a suitable normalization scheme. Recalling that $\varepsilon_i = 0.2(a/R)$ and R is fixed in this work, the parameter that controls ε_i is the contact radius at the onset of creep a_0, which is the appropriate length scale for normalizing h_{creep}.

Figure 3b shows the variation in h_{creep}/a_0 as a function of ε_i. In the fig. the elastic and plastic regimes are demarcated on the basis of the quasi-static indentation results (see Fig. 1a). While h_{creep}/a_0 increased with ε_i over the entire range of ε_i investigated in this work, the rate of change in h_{creep}/a_0 with ε_i was significantly larger when the material transitted into the plastic regime. While the data for the BMGs appear to collapse onto a single line within the elastic regime, h_{creep}/a_0 for $Cu_{50}Zr_{50}$ was markedly higher than that for $Cu_{65}Zr_{35}$ in the plastic regime. Also, the difference appeared to increase with increasing ε_i.

Although the detailed mechanism for these two observations, (i) h_{creep}/a_0 vs. ε_i and (ii) the difference in h_{creep}/a_0 between the two alloys, is not yet fully understood, a hypothesis was possible based on the assumption that the amount of creep deformation was strongly dependent on the BMG structural state at the onset of creep, i.e. a BMG having a larger free volume will show more pronounced creep deformation due to the operation of STZs [2,3]. A larger amount of initial free volume can result in the occurrence of more STZs and, thus, a BMG having a lower free volume would exhibit higher resistance to plastic deformation (i.e. a higher hardness as well as creep resistance).

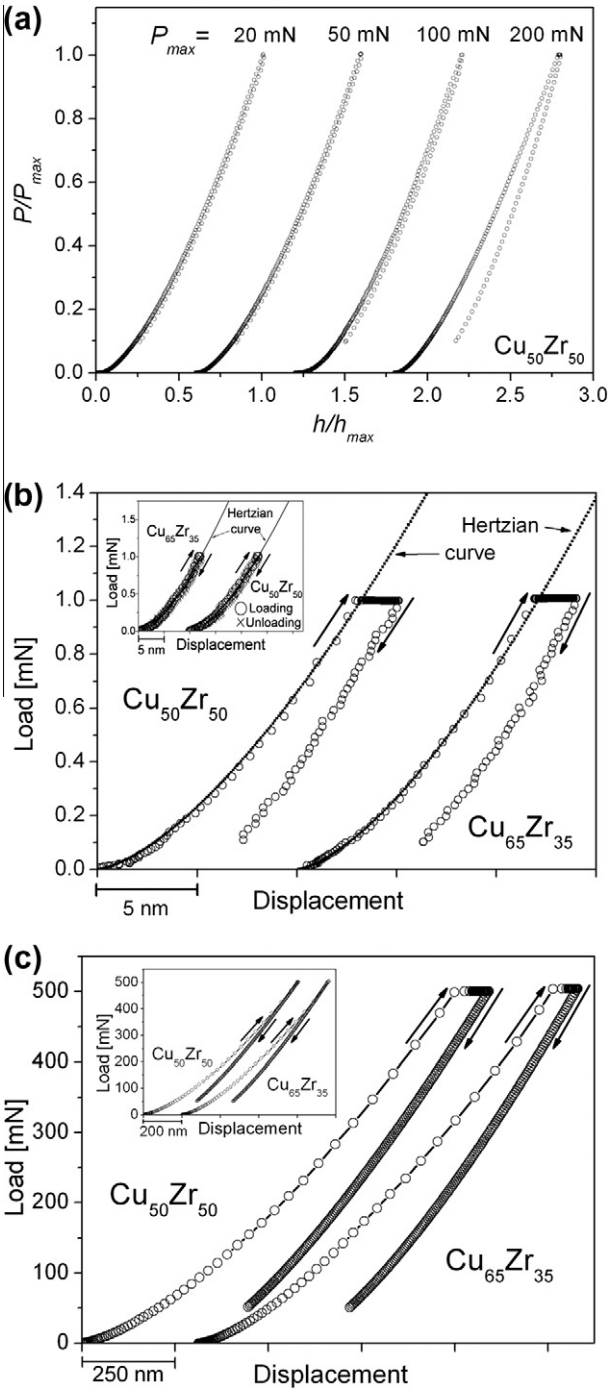

Figure 1. Representative load–displacement (P–h) curves obtained from spherical indentation. (a) Normalized curve recorded during quasi-static indentation of $Cu_{50}Zr_{50}$ alloy at different P_{max} under a constant strain rate of $0.1\,s^{-1}$. (b) Indentation creep curve for $P_{max} = 1$ mN (the lowest load). Hertzian elastic curves are also drawn for comparison. (c) Indentation creep curve for $P_{max} = 500$ mN (the highest load). Inset images in (b) and (c) show the quasi-static indentation curves obtained at the same maximum load.

To understand the influence of ε_i on creep deformation, possible structural changes that occurred during loading need to be identified. When the applied stress is elastic the STZs or other defects responsible for plastic deformation may not operate. However, this does not mean the absence of structural change. Recent studies

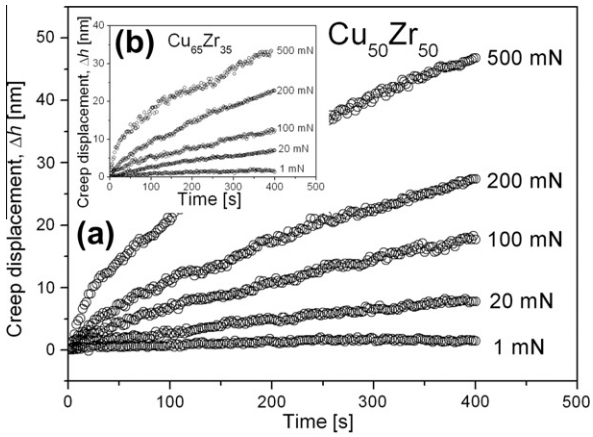

Figure 2. Representative creep displacement vs. time curves obtained at different holding loads. (a) $Cu_{50}Zr_{50}$. (b) $Cu_{65}Zr_{35}$.

[4,6,10] proposed that elasto-static stress can induce a small amount of "structural disorder" (whose size may be much smaller than typical STZs), which in turn leads to the creation of excess free volume. Park et al. [10] claimed that the degree of disordering was larger in BMGs that had higher atomic packing densities (or lower initial free volumes) due to their higher energetic stability and greater energy absorption capability. If this is true, a smaller amount of the excess free volume can be generated in $Cu_{50}Zr_{50}$ (having a higher amount of initial free volume) than $Cu_{65}Zr_{35}$. Therefore, at the onset of creep $Cu_{65}Zr_{35}$ and $Cu_{50}Zr_{50}$ could have a similar amount of total free volume and in turn exhibit a similar amount of creep deformation. This rationalizes the observed compositional independence of creep within the elastic regime.

We now turn our attention to creep for the case where $\varepsilon_i > \varepsilon_y$. It is well established that macroscopic "plastic" deformation of metallic glasses through shear banding leads to flow softening [19–21]. Further, it has been shown that extensive shear band-mediated plastic flow can occur underneath the indenter [22]. The micromechanism responsible for this is the substantial amount of excess free volume that is created during the operation of STZs [2,3]. The substantial increase in free volume content that occurs during the loading sequence of spherical indentation aids the consequent operation of the STZs during creep deformation. This is the reason for the observation of accelerated creep rates in the plastic regime. Since STZs are sensitive to both the initial free volume content and the amount of plastic deformation, $Cu_{50}Zr_{50}$ (having a greater operation of STZs or free volume coalescence) would be expected to show larger creep deformation than $Cu_{65}Zr_{35}$, and the difference may increase with ε_i. This is supported by a recent study on cold rolling of BMGs in which it was reported that the free volume content increased with increasing plastic strain [23].

In summary, the room temperature time-dependent deformation behavior of two Cu–Zr BMGs as a function of the initial strain imposed was investigated by employing the spherical nanoindentation technique. The experimental results showed that creep occurred homogeneously in both alloys. The amount of deforma-

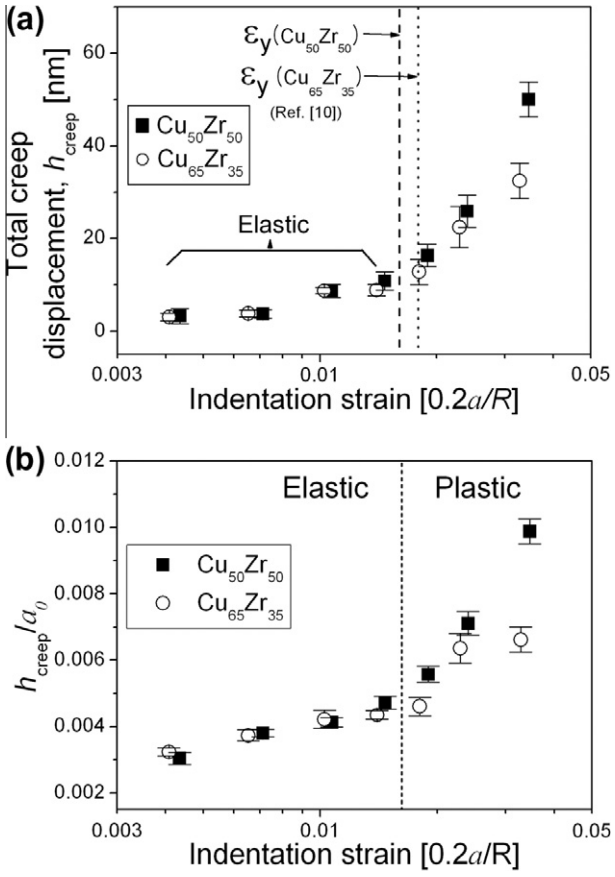

Figure 3. Variation in total creep displacement as a function of the indentation strain. (a) Total creep displacement. (b) The adjusted creep displacement.

tion was found to be sensitive to ε_i. A small yet linear increase, which was independent of the composition, in creep amount was observed within the elastic regime. When ε_i transitted to the plastic regime the creep rates increased significantly. They then depended on the initial free volume content of the material.

This work was supported by the Human Resources Development Program of the Korea Institute of Energy Technology Evaluation and Planning (KETEP), grant funded by the Korean government Ministry of Knowledge Economy (2008-P-EP-HM-E-04-0000). The authors thank Ms. Kyoung-Won Park (KIST) for providing the valuable samples.

[1] F. Spaepen, Acta Metall. 25 (1977) 407.
[2] A.S. Argon, Acta Metall. 27 (1979) 47.
[3] C.A. Schuh, T.C. Hufnagel, U. Ramamurty, Acta Mater. 55 (2007) 4067.
[4] M.L. Falk, J.S. Langer, Phys. Rev. E 57 (1998) 7192.
[5] M. Heggen, F. Spaepen, M. Feuerbacher, J. Appl. Phys. 97 (2005) 033506.
[6] F. Albano, M.L. Falk, J. Chem. Phys. 122 (2005) 154508.
[7] S.-J. Lee, B.-G. Yoo, J.-I. Jang, J.-C. Lee, Met. Mater. Int. 14 (2008) 9.
[8] W.H. Li, K. Shin, C.G. Lee, B.C. Wei, T.H. Zhang, Y.Z. He, Mater. Sci. Eng. A 478 (2008) 371.
[9] A. Castellero, B. Moser, D.I. Uhlenhaut, F.H. Dalla Torre, J.F. Löffler, Acta Mater. 56 (2008) 3777.
[10] K.-W. Park, C.-M. Lee, M. Wakeda, Y. Shbutani, M.L. Falk, J.-C. Lee, Acta Mater. 56 (2008) 5440.
[11] K.-W. Park, C.-M. Lee, J.-C. Lee, J. Kor, Inst. Met. Mater. 47 (2009) 759.
[12] Y.J. Huang, Y.L. Chiu, J. Shen, J.J.J. Chen, J.F. Sun, J. Mater. Res. 24 (2009) 978.
[13] Y.J. Huang, J. Shen, Y.L. Chiu, J.J.J. Chen, J.F. Sun, Intermetallics 17 (2009) 190.
[14] B.-G. Yoo, J.-H. Oh, Y.-J. Kim, K.-W. Park, J.-C. Lee, J.-I. Jang, Intermetallics 18 (2010) 1898.
[15] K.L. Johnson, Contact Mechanics Cambridge, Cambridge University Press, UK, 1985.
[16] W.C. Oliver, G.M. Pharr, J. Mater. Res. 19 (2004) 3.
[17] N. Mattern, J. Bednarčik, S. Pauly, G. Wang, J. Das, J. Eckert, Acta Mater. 57 (2009) 4133.
[18] J.-I. Jang, B.-G. Yoo, J.-Y. Kim, Appl. Phys. Lett. 90 (2007) 211906.
[19] R. Bhowmick, R. Raghavan, K. Chattopadhyay, U. Ramamurty, Acta Mater. 54 (2006) 4221.
[20] B.-G. Yoo, K.-W. Park, J.-C. Lee, U. Ramamurty, J.-I. Jang, J. Mater. Res. 24 (2009) 1405.
[21] B.-G. Yoo, Y.-J. Kim, J.-H. Oh, U. Ramamurty, J.-I. Jang, Scripta Mater. 61 (2009) 951.
[22] U. Ramamurty, S. Jana, Y. Kawamura, K. Chattopadhyay, Acta Mater. 53 (2005) 705.
[23] J.W. Liu, Q.P. Cao, L.Y. Chen, X.D. Wang, J.Z. Jiang, Acta Mater. 58 (2010) 4827.